Received: 10 April 2021 | Revised: 2 August 2021 | Accepted: 14 September 2021 | Published on: 27 September 2021

DOI: 10.1111/tra.12818

RESEARCH ARTICLE

Traffic WILEY

Secretion of a low-molecular-weight species of endogenous GRP94 devoid of the KDEL motif during endoplasmic reticulum stress in Chinese hamster ovary cells

Andrew Samy[1] | Noriko Yamano-Adachi[1,2] | Yuichi Koga[1,2] | Takeshi Omasa[1,2]

[1]Department of Biotechnology, Graduate School of Engineering, Osaka University, Suita, Japan

[2]Industrial Biotechnology Initiative Division, Institute for Open and Transdisciplinary Research Initiatives, Osaka University, Suita, Japan

Correspondence
Takeshi Omasa, Ph.D., Department of Biotechnology, Graduate School of Engineering, Osaka University, 2-1 Yamadaoka, Suita, Osaka 565-0871 Japan.
Email: omasa@bio.eng.osaka-u.ac.jp

Funding information
MEXT/JSPS KAKENHI, Grant/Award Number: JP17H06157; Japan Agency for Medical Research and Development, Grant/Award Numbers: JP20ae0101066, JP20ae0101058, JP20ae0101057, JP20ae0101056, JP17ae0101003

Abstract

GRP94 (glucose-regulated protein 94) is a well-studied chaperone with a lysine, aspartic acid, glutamic acid and leucine (KDEL) motif at its C-terminal, which is responsible for GRP94 localization in the endoplasmic reticulum (ER). GRP94 is upregulated during ER stress to help fold unfolded proteins or direct proteins to ER-associated degradation. In a previous study, engineered GRP94 without the KDEL motif stimulated a powerful immune response in vaccine cells. In this report, we show that endogenous GRP94 is naturally secreted into the medium in a truncated form that lacks the KDEL motif in Chinese hamster ovary cells. The secretion of the truncated form of GRP94 was stimulated by the induction of ER stress. These truncations prevent GRP94 recognition by KDEL receptors and retention inside the cell. This study sheds light on a potential trafficking phenomenon during the unfolded protein response that may help understand the functional role of GRP94 as a trafficking molecule.

KEYWORDS
endoplasmic reticulum, ER stress, GRP94, heat shock protein, KDEL motif, protein secretion, trafficking, unfolded protein response

1 | INTRODUCTION

HSPs are highly conserved molecular chaperones responsible for folding, intracellular transport and refolding or degradation of misfolded proteins.[1] HSPs localize in the nucleus, ER, cytosol and mitochondria.[2,3] They are classified by either their molecular weight or their dependence on ATP.[1,4] According to their size, HSPs are divided into Hsp100, Hsp90, Hsp70, Hsp60 and the small HSPs. Small HSPs are ATP-independent, whereas larger HSPs hydrolyze ATP, which leads to their conformational change and interaction with substrates.[4]

In mammalian cells, HSP90s are a group of four paralogs distributed throughout the cell, with GRP94 (glucose-regulated protein 94) found in the ER, Hsp90α and β in the cytosol (isoforms) and TRAP1 (tumor necrosis factor receptor-associated protein 1) in mitochondria.[5,6] GRP94 is a well-studied HSP chaperone that resides in the ER because of the C-terminal KDEL motif. This member of the HSP90 family[2,5,7] consists of three main domains: an N-terminal domain responsible for ATPase activity, a middle domain responsible for

Abbreviations: BFA, brefeldin A; BiP, binding immunoglobulin protein; CHO, Chinese hamster ovary; CHOP, C/EBP homologous protein; CMV, cytomegalovirus; DMSO, dimethyl sulphoxide; ER, endoplasmic reticulum; ERAD, ER-associated degradation; FBS, fetal bovine serum; FT, flow through; GRP94, glucose-regulated protein 94; HC, heavy chain; HSP, heat shock protein; IP, immunoprecipitation; IgG, immunoglobulin G; KDEL, lysine, aspartic acid, glutamic acid and leucine motif; LC, light chain; mAb, monoclonal antibody; PBS, phosphate-buffered saline; PDI, protein disulfide isomerase; PTMs, post-translational modifications; UPR, unfolded protein response; VCD, viable cell density.

ligand binding, and a C-terminal domain responsible for dimerization.[2] The N-terminal domain is preceded by a pre-N domain, which plays a role in GRP94 client maturation and regulation of the rate of ATP hydrolysis.[5,8] The sequence of the pre-N domain of GRP94 from human and canine is composed predominantly of charged amino acids, making this domain a proteolytically sensitive region.[9] GRP94 and Hsp90 are active upon forming a homodimer,[10] and although being the most abundant protein in the ER, GRP94 interacts very selectively with specific clients.[2,11] For example, GRP94 interacts with immunoglobulin heavy and light chains and insulin-like proteins.[11] It

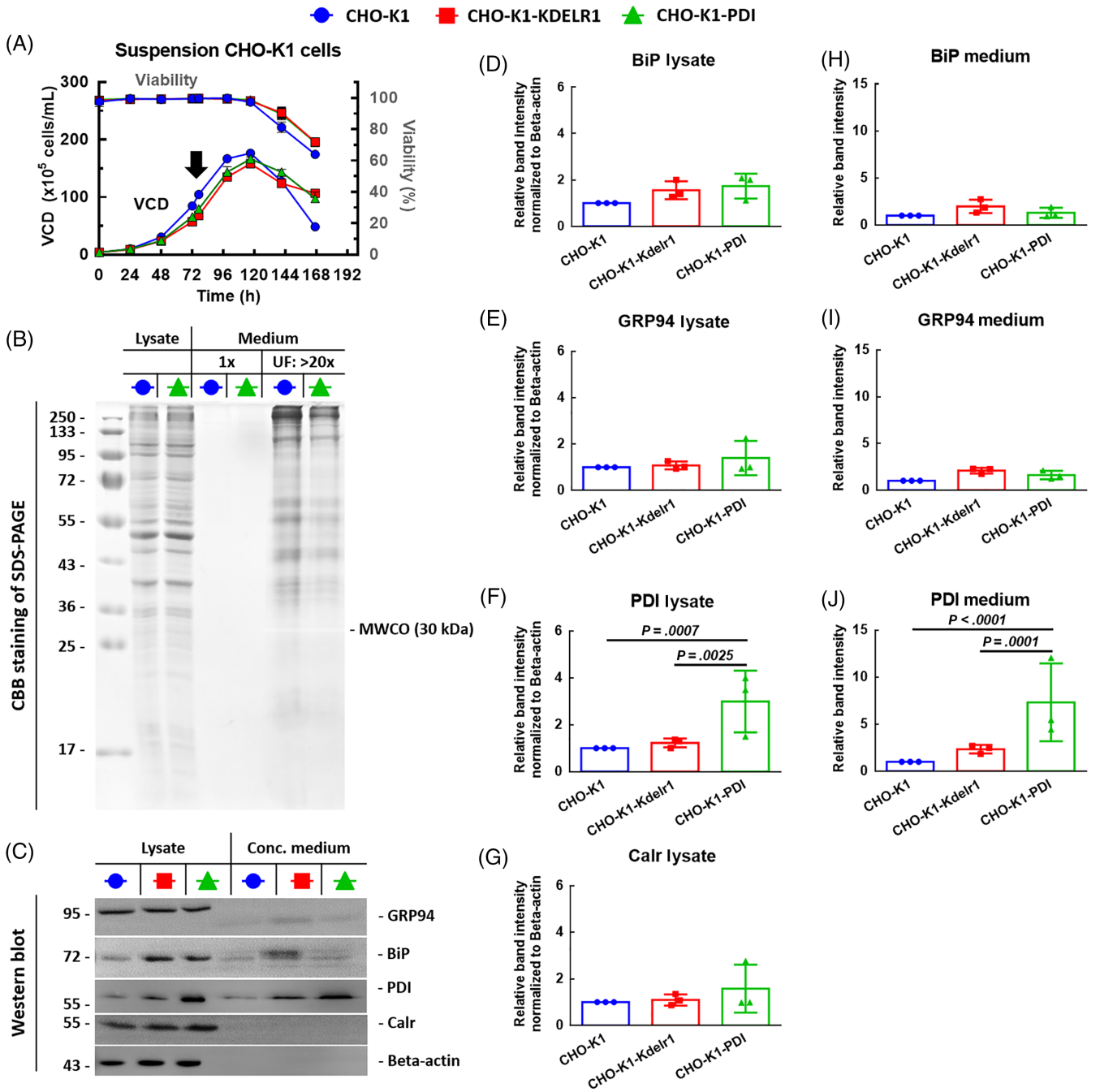

FIGURE 1 Soluble ER chaperones are secreted into the extracellular medium. (A) CHO-K1 suspension batch cultures showing the viable cell density and viability of the cells. The black arrow indicates the sampling time point during the exponential growth phase of the cultures. (B) CBB-stained 12% SDS-PAGE gel showing the results for lysate samples, medium samples and samples of concentrated medium prepared by ultracentrifugation using a 30 kDa molecular weight cut-off (MWCO) membrane. (C) Western blot of lysate samples and samples of concentrated medium against ER chaperone proteins BiP, PDI, Calr and GRP94. (D-G) Relative band intensity analysis normalized to β-actin and to CHO-K1 cells as a control cell lysate sample. (D) BiP, (E) GRP94, (F) PDI and (G) Calr. (H-J) Relative band intensity analysis of a sample of concentrated medium normalized to CHO-K1 cells as control samples showing (H) BiP, (I) GRP94 and (J) PDI. Statistical analysis was performed using Tukey's multiple comparison test. $P < .05$ was considered to reflect a statistically significant difference. VCD, viable cell density

plays important roles in protein folding and ER quality control, specifically in the ERAD pathway.[2,12]

The UPR is a mechanism of cell defense against conditions in which proteins have accumulated in the ER because of changes in intracellular pH, calcium ion concentrations, variations in culture temperature or exposure to chemicals. The UPR upregulates and/or activates several transcription factors that mediate the upregulation of ER chaperones and other intermediate molecules that enable the cell to correctly fold or degrade proteins that have accumulated in the ER.[13,14] This cellular response ensures that cells return to homeostasis, and studies have shown that the UPR and glucose-regulated proteins play roles in maintaining organ homeostasis.[15,16]

The CHO cell line is widely used in the production of biopharmaceuticals because CHO cells grow readily in serum-free medium, cultures can be upscaled to hundreds of liters, and recombinant proteins can be produced that have PTMs resembling those of human PTMs. CHO cells have been studied in different research fields including cell engineering,[17-20] transcriptomics,[21] metabolomics,[22-24] and genomics.[25] Despite extensive research having been conducted on CHO cells, more research is required to further understand the biology of these cells in order to open new gateways for cell engineering.

GRP94 has one of the highest mRNA counts in recombinant CHO cells.[26] Moreover, similar to BiP, GRP94 is highly upregulated during UPR activation and late-stage batch cultures.[20,26,27] In our recent study, we showed that the gene expression levels of KDEL chaperones and receptors in CHO cells are not upregulated in a coordinated manner during the induction of ER stress.[20]

In this study, while investigating the possibility of saturating the ER retention machinery, we discovered that GRP94 is secreted into the extracellular medium as a truncated molecular species in CHO cells,

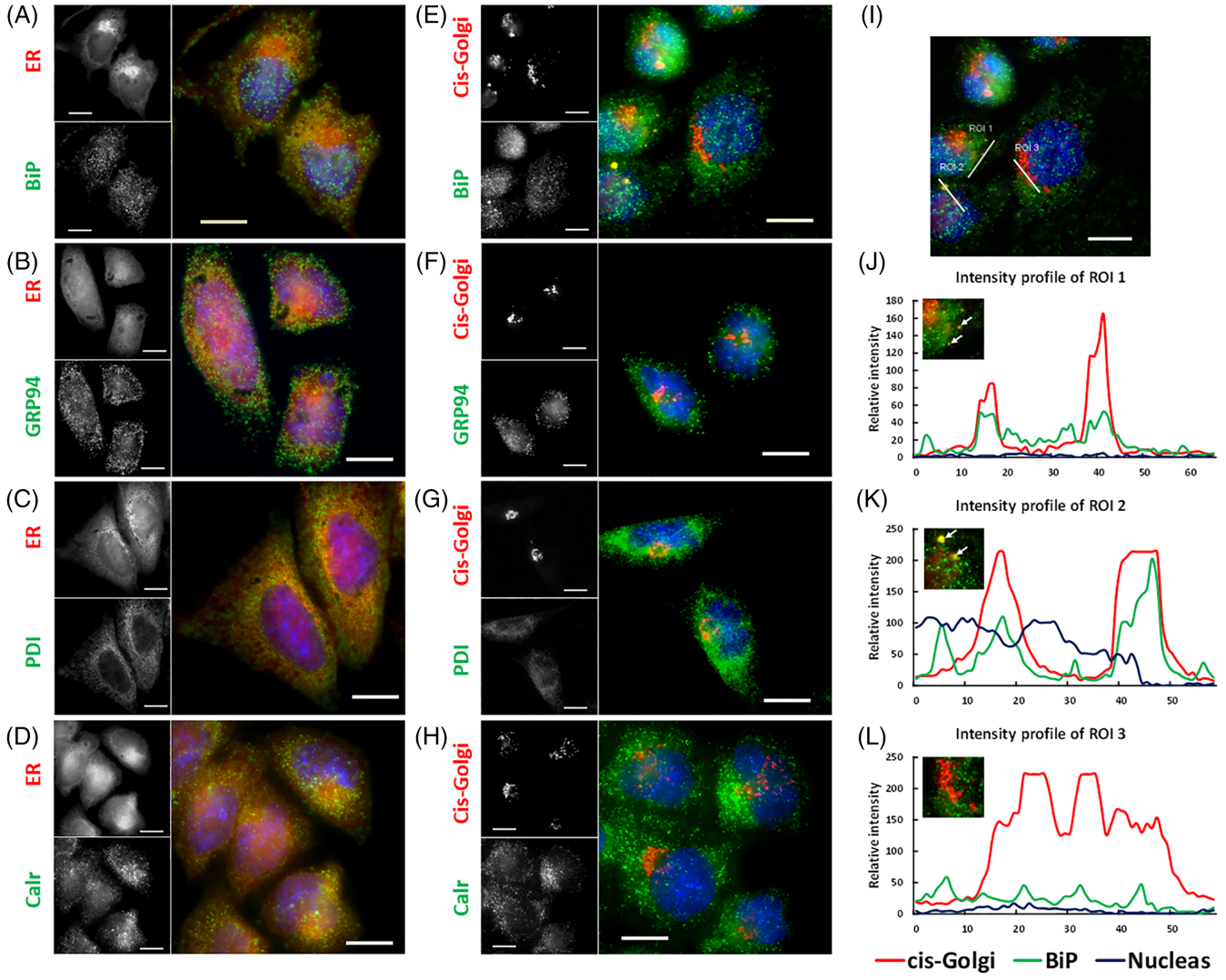

FIGURE 2 Localization of the four KDEL chaperones in the ER and *cis*-Golgi by immunofluorescence. CHO-K1 cells grown on precoated coverslips in 12-well plates were fixed and immunostained by antibodies specific for each of the four chaperones against the ER marker (ER-ID dye): (A) BiP, (B) GRP94, (C) PDI and (D) Calr or anti-GM130 as a *cis*-Golgi marker: (E) BiP, (F) GRP94, (G) PDI and (H) Calr. Cells were captured using a 100× oil lens and approximately 50-60 cells from four to seven fluorescent images were counted and checked for localization in the *cis*-Golgi and ER. Among the observed cells, GRP94 did not localize in the *cis*-Golgi. An example of *cis*-Golgi localization of (I) BiP with three regions of interest showing localization indicated by white arrows (J,K) or no localization (L). Scale bar is 10 μm

unlike the other three KDEL motif-bearing chaperones, BiP, calreticulin and PDI. Production of this truncated form of GRP94 was induced by ER stress. This led us to deliberate over the importance of GRP94 as a trafficking molecule or as an extracellular antigen-presenting HSP.[28,29] Accordingly, we studied the truncated form of GRP94 and investigated whether this form retains the ER retention motif.

2 | RESULTS

2.1 | Overexpression of PDI promotes its secretion into the culture medium

CHO-K1 cells overexpressing KDELR1 (KDEL receptor 1) or PDI (family member 1, KDEL chaperone) were engineered to investigate the possibility of saturating the ER retention machinery and the secretion of ER chaperones into the medium. CHO-K1 cells overexpressing either KDELR1 or PDI were grown in batch cultures (Figure 1A). Cell samples were taken during the exponential growth phase, and both cell lysates and samples of concentrated medium were analyzed by SDS-PAGE. Medium samples were concentrated by ultrafiltration using 30-kDa molecular weight cut-off (MWCO) membranes (Figure 1B). Samples were blotted onto PVDF membranes and probed against KDEL chaperones (ie, GRP94, BiP, Calr and PDI) (Figure 1C). Cells overexpressing KDELR1 did not show any improved retention in cell lysates (Figure 1D-G) or secretion into the medium (Figure 1H-J) of the KDEL chaperones. However, cells overexpressing PDI (CHO-K1-PDI) showed a significant increase in the signal of band intensity of PDI in both the lysate (Figure 1F) and the sample of concentrated medium (Figure 1J) when compared with those of the parental CHO-K1 cells and CHO-K1-KDELR1 cells. Calreticulin was not released into the medium or the amount released was below the detection limit. Notably, GRP94 was secreted into the medium as a species with a lower molecular weight (ie, 75-86 kDa) than that of full-length GRP94 present in the cell lysate.

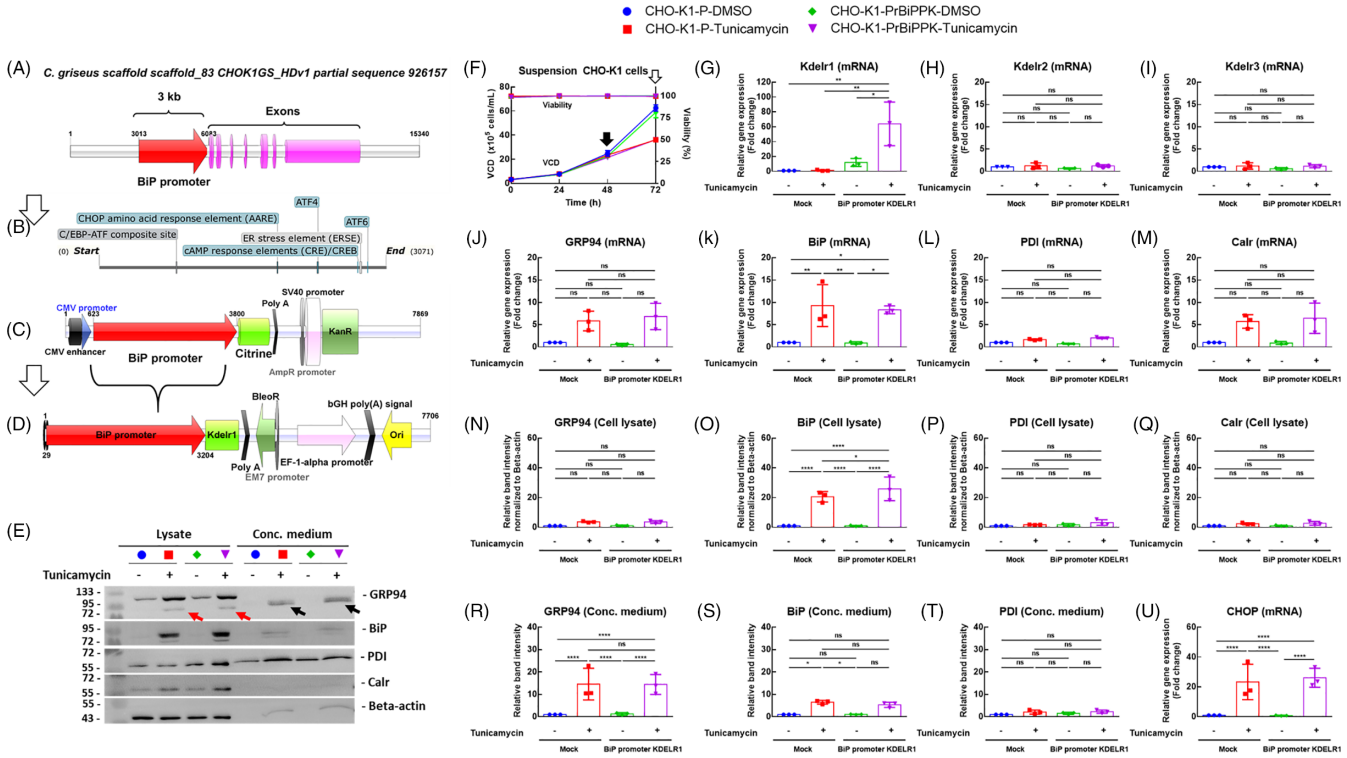

FIGURE 3 Secretion of GRP94 into the medium as a low-molecular-weight species independent of KDELR1. (A) Scheme showing the Hspa5 gene (expressing BiP) in the CHO-K1 genome with the 3-kb BiP promoter upstream of the transcription start site. (B) Alignment of the ER stress elements on the cloned promoter length. (C) The 3-kb BiP promoter was cloned into the pcDNA3.1 plasmid and upstream of citrine. (D) The BiP promoter was cloned upstream of KDELR1 in the pBudCE4.1-KDELR1 plasmid. (E) Lysates and samples of concentrated medium were blotted against the four chaperones (GRP94, BiP, PDI and Calr) and β-actin. Red arrows represent the truncated form of GRP94 induced by ER stress. Black arrows indicate the truncated form of GRP94 that is secreted into the medium during ER stress. CHO-K1 cells were transfected with the mock plasmid or with the engineered model (CHO-K1-PrBiP-KDELR1). (F) ER stress was induced by the addition of 5 μg/mL tunicamycin during the exponential growth phase of the suspension batch culture. Black arrow indicates when ER stress was induced, while white arrow indicates the sampling time point and when medium samples were concentrated. Relative gene expression was measured by RT-qPCR with normalization to the β-actin gene: (G) Kdelr1, (H) Kdelr2, (I) Kdelr3, (J) GRP94, (K) BiP, (L) PDI, (M) Calr and (U) CHOP. Lysates' relative band intensities were normalized to β-actin and to a mock CHO-K1 cell sample with vehicle treatment: (N) GRP94, (O) BiP, (P) PDI and (Q) Calr. Concentrated medium samples were normalized to the same CHO-K1 control sample: (R) GRP94, (S) BiP and (T) PDI. Error bars represent mean and SD of three independent experiments of the same engineered cell pool. Statistical analysis was performed using Tukey's multiple comparison test. $P < .05$ was considered significant (*<.05, **<.01, ****<.0001). The engineered Kdelr1 mRNA values were calculated separately from the other mRNA results

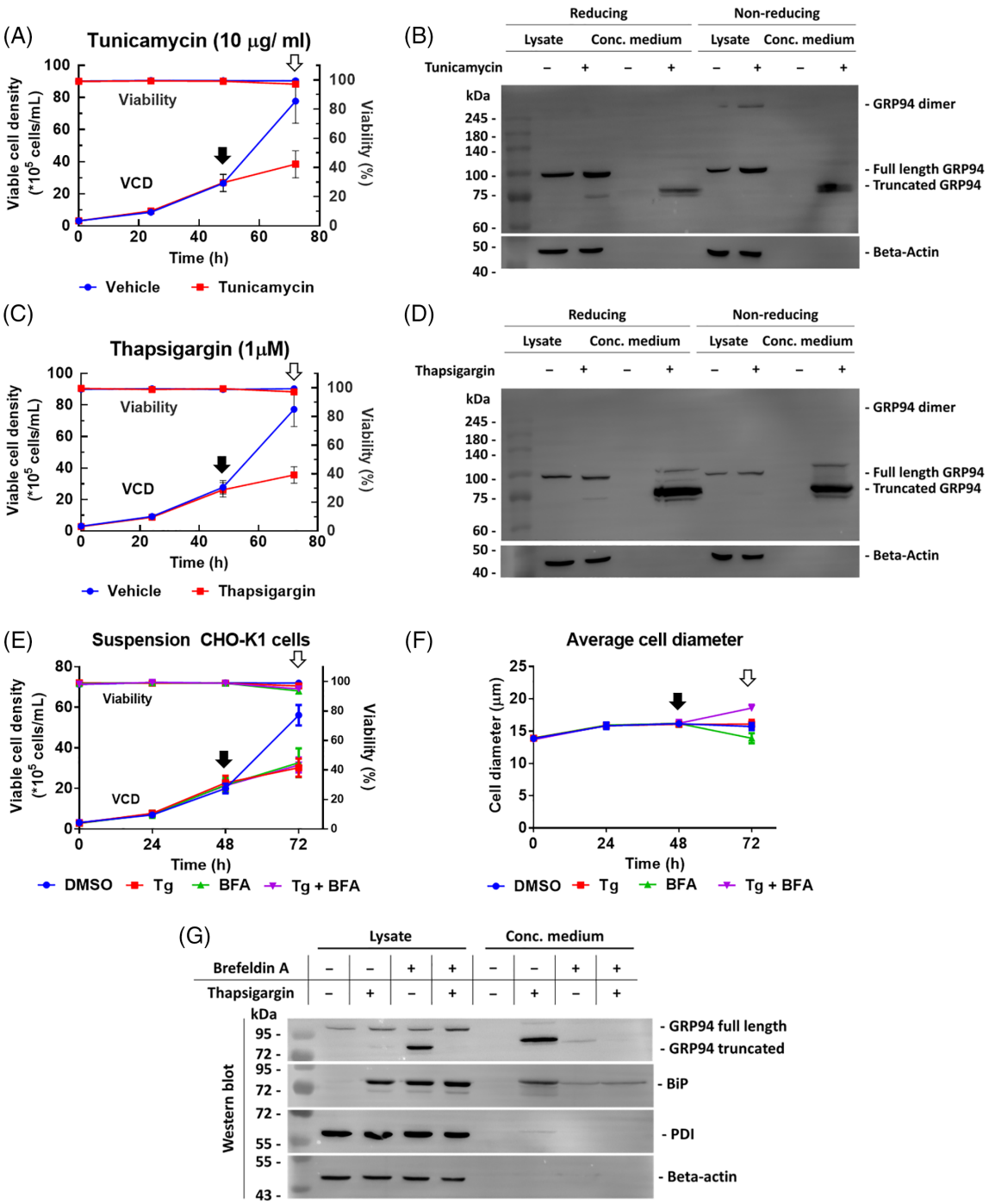

FIGURE 4 GRP94 is secreted into the medium through the canonical ER to Golgi pathway. (A,B) ER stress induced by 10 μg/mL tunicamycin for 24 hours. (A) Viable cell density and (B) western blot of GRP94 in a cell lysate and concentrated medium under reducing and nonreducing conditions. (C,D) ER stress induced by 1 μM Tg for 24 hours. (C) Viable cell density and (D) western blot of GRP94 in a cell lysate and concentrated medium under reducing and nonreducing conditions. (E-G) Treatment of CHO-K1 with Tg, BFA or both. (E) Viable cell density. (F) Average diameter of cells measured automatically using ViCell counter. (G) Western blot of GRP94, BiP, PDI and β-actin in cell lysate and concentrated medium showing that the active secretion of GRP94 and BiP was blocked by BFA treatment and they accumulated inside the cell. Black arrows indicate the time point when ER stress was induced, whereas white arrows indicate the time point when cell and medium samples were taken. Experiments were performed independently two times

2.2 | GRP94 does not reside in the *cis*-Golgi unlike other KDEL chaperones

Adherent CHO-K1 cells were fixed on lysine-coated coverslips and immunostained by antibodies against the four KDEL chaperones (GRP94, BiP, Calr and PDI) to detect their localization with the ER and *cis*-Golgi (Figure 2A-H). Four to seven images containing 50 to 60 cells were examined to detect whether the chaperones are located in the *cis*-Golgi. Cells showing overlap between the green (chaperones) and red (*cis*-Golgi) channels indicated colocalization (colored yellow in

Figure 2). BiP, PDI and Calr showed *cis*-Golgi localization. In contrast, all observed cells in GRP94-stained samples showed no *cis*-Golgi localization, as reported previously for human endothelial EAhy926 cells.[30] The four chaperones localized to the ER in all cells, as expected. Examples of localization and the absence of localization are shown in Figure 2I-L. Regions of interest are marked on the image (Figure 2I) and the intensity profiles of the three channels were measured. Similar patterns between the green (chaperones) and red (*cis*-Golgi) channels indicated localization of the chaperones in the *cis*-Golgi compartment. GRP94 showed localization with anti-KDEL antibody during normal and ER stress conditions. Additionally, GRP94 migrated to the cell membrane when ER stress was induced in adherent CHO-K1 cells by 5 μg/mL tunicamycin, indicating that the KDEL motif of GRP94 was either truncated or masked (Figure S1).

2.3 | GRP94 is secreted into the medium as a low-molecular-weight species during ER stress independent of KDELR1

To better understand the dependence of chaperone secretion on KDELR1 expression, KDELR1 under the BiP promoter was expressed and ER stress was then induced.

Three kilobases of the BiP promoter upstream of the transcription start site was cloned (Figure 3A) after defining the size of this promoter by aligning the known transcription factor binding sites (Figure 3B). This 3 kb BiP promoter sequence was cloned into the pcDNA3.1 plasmid upstream of citrine (GFP variant) (Figure 3C) and then cloned into the previously constructed pBudCE4.1-KDELR1 plasmid[20] to replace the CMV promoter (Figure 3D). A suspension batch culture (Figure 3F) was grown, samples of which were taken for RT-qPCR and western blot analysis (Figure 3E). The engineered cell model expressing KDELR1 under the BiP promoter showed the expected upregulation of KDELR1 upon the induction of ER stress (Figure 3G). Quantitative RT-PCR of *Kdelr2* and *Kdelr3* showed minimal upregulation in mock and engineered cell lines (Figure 3H-I). Genes encoding GRP94, PDI and Calr showed upregulation, albeit not significantly, whereas that encoding BiP showed significant upregulation (Figure 3J-M). Western blots of cell lysates (Figure 3N-Q) and concentrated culture supernatants (Figure 3R-T) were measured to compare BiP and GRP94 specifically. GRP94 showed moderate but insignificant upregulation in cell lysates (Figure 3N) and a significant level of secretion (Figure 3R) into the medium during ER stress in both cell lines. In contrast, BiP showed significant upregulation in cell lysates and improved retention in the engineered model in comparison with the mock cell during ER stress (Figure 3O). BiP also showed significant secretion into the medium (Figure 3S) in the mock cell line, but such secretion did not reach significance in the BiP promoter-KDELR1 engineered cell model. The gene encoding CHOP (C/EBP Homologous Protein) showed significant gene upregulation in both cell lines (Figure 3U). GRP94 was secreted during ER stress as a low-molecular-weight species, as shown in Figure 3E (black arrows). Interestingly, the low-molecular-weight GRP94 species was also found to be induced intracellularly upon the induction of ER stress (red arrows). This suggests that a low-molecular-weight species of GRP94 arises intracellularly during ER stress, which is then secreted into the extracellular medium in a KDELR1-independent manner.

2.4 | GRP94 is secreted into the medium through the canonical ER to Golgi pathway

To understand the process of secretion of GRP94 during stress conditions in CHO cells, we treated these cells with either tunicamycin (Figure 4A,B) or thapsigargin (Tg, Figure 4C,D). Samples were treated with reducing or nonreducing sample buffers and subjected to SDS-PAGE. GRP94 was found to be expressed as both a monomer and a dimer intracellularly, as shown in Figures 4B and S2. We then treated CHO cells with Tg, BFA or both to investigate the pathway of secretion into the medium (Figure 4E). BFA was found to induce ER stress in a manner similar to Tg, as demonstrated by the upregulation of BiP, as shown in Figure 4G. Treatment with BFA alone induced the intracellular accumulation of low-molecular-weight GRP94 and prevented its secretion into the medium. Additionally, BiP secretion into the medium was inhibited by treatment with BFA. Surprisingly, co-treatment with Tg/BFA induced neither the accumulation of the low-molecular-weight species of GRP94 nor its secretion. Upon co-treatment, the cell diameter was found to increase, when measured with a ViCell counter (Figure 4F). These results collectively

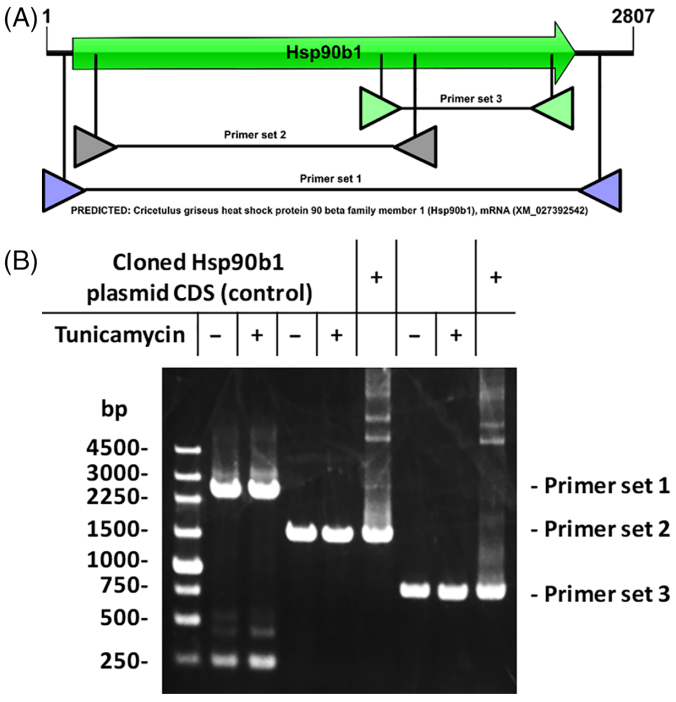

FIGURE 5 Low-molecular-weight GRP94 is not a transcript variant. ER stress was induced, total mRNA was extracted, cDNA was synthesized and then PCR was run using three primer sets. The results did not show any smaller size band in tunicamycin-treated samples. (A) mRNA transcript of Hsp90b1 showing the location of the designed primers. (B) Agarose gel electrophoresis of the PCR products

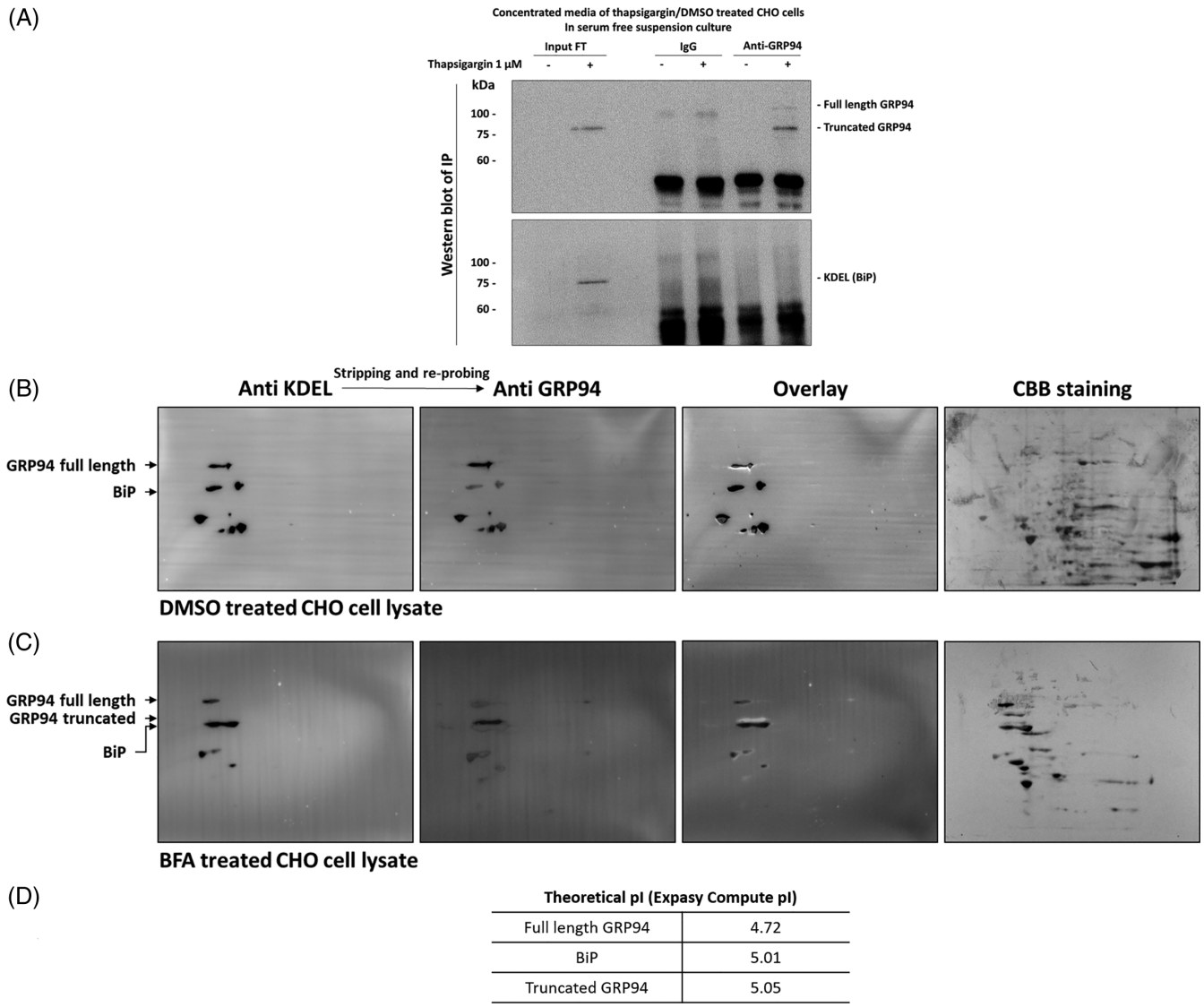

(D)

Theoretical pI (Expasy Compute pI)	
Full length GRP94	4.72
BiP	5.01
Truncated GRP94	5.05

FIGURE 6 Low-molecular-weight GRP94 is devoid of the KDEL motif. (A) Western blot of IP of concentrated media after treating samples with either DMSO or inducing ER stress by Tg and probing against GRP94 (top) and KDEL (bottom), (B,C) 2D gel electrophoresis of DMSO (B) or BFA (C) treated CHO-K1 cell lysates while probing against KDEL, stripping and reprobing against GRP94 and then staining the membrane with CBB. The anti-KDEL and anti-GRP94 images were overlaid in both samples. (D) Theoretical isoelectric point calculation of full-length GRP94, BiP and GRP94 after losing its acidic C-terminal

suggest that the low-molecular-weight species of GRP94 originates in the ER and is secreted out of the cell through the canonical ER to Golgi pathway.

2.5 | Low-molecular-weight GRP94 is not a transcript variant of the same gene

In the CHO genome database, there are no reported transcript variants of GRP94. To investigate this experimentally, we treated cells with tunicamycin, extracted total RNA, synthesized cDNA, and then performed RT-PCR. We designed three primer sets that cover the mRNA transcript of Hsp90b1 (gene expressing GRP94) (Figure 5A). We then subjected the PCR products to agarose gel electrophoresis, as shown in Figure 5B. We did not observe extra bands equivalent to the predicted size of the low-molecular-weight protein upon comparing the vehicle-treated and tunicamycin-treated samples. These results suggest that the low-molecular-weight GRP94 is a result of processing at the protein level and not at the mRNA level.

2.6 | GRP94 loses its acidic C-terminal and KDEL ER retention motif during secretion and ER stress induction

To further investigate the truncated form of GRP94, ER stress was induced by Tg. We immunoprecipitated GRP94 from concentrated medium samples of DMSO-treated and Tg-treated cells (Figure 6A). The flow-through showed one intense low molecular weight species

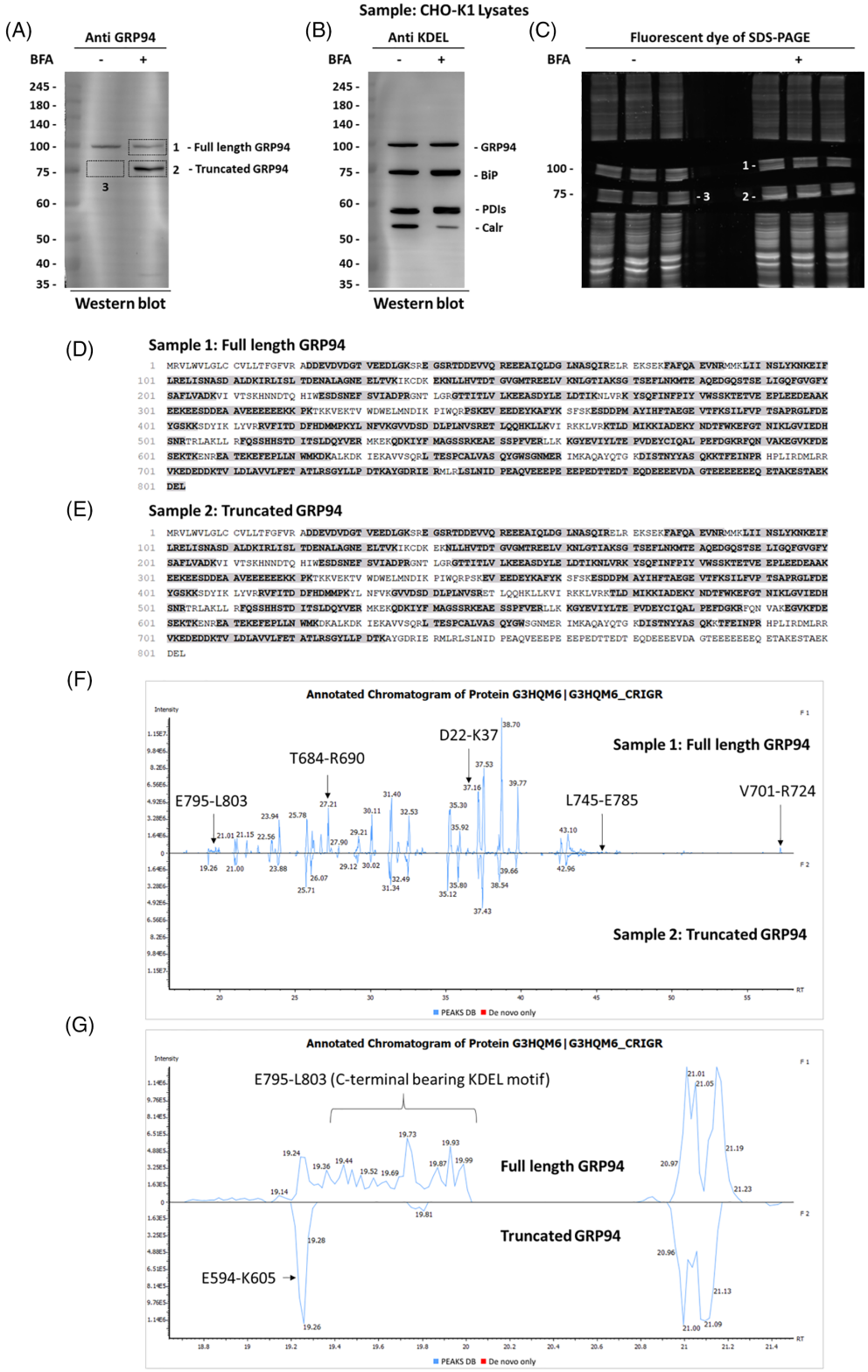

FIGURE 7 Mass spectroscopy analysis of GRP94 in medium shows very low abundance of its acidic C-terminal. Cell lysate samples of BFA-treated CHO-K1 cells were run on two 8% gels. The first was blotted against GRP94 (A) and KDEL (B), while the second was stained by SYPRO Ruby protein gel stain, the gel was cut in molecular weight around 75 and 100 kDa (C) and sent for peptide mapping. (D) Sequence coverage of full length GRP94 (samlpe1) in BFA-treated CHO cell lysates. (E) Sequence coverage of truncated GRP94 (sample 2) in BFA-treated CHO cell lysates. (F) Stacked peptide maps of full length (top) and truncated (bottom) GRP94. (G) Zoomed region of retention time of 19-21 minutes at which the E795-L803 C-terminal peptide containing KDEL motif appears. The peaks appear in the full length GRP94 (top) while in the truncated GRP94 (bottom) sample they seem to be missing

GRP94 band. The immunoprecipitated GRP94 showed a faint GRP94 full-length band and a dense truncated form when blotted against GRP94. This small molecular weight species was not detected by anti-KDEL antibody. The C-terminal tail of GRP94 is highly acidic and disordered. Accordingly, we hypothesized that the truncated form does not have the KDEL retention motif. We subjected the DMSO-treated and BFA-treated cell lysates to 2D gel electrophoresis, performed blotting against KDEL, and then stripped and reprobed the membrane against GRP94 (Figure 6B-C). The low-molecular-weight GRP94 was not detected by anti-KDEL antibody, as shown in Figure 6C. The theoretical isoelectric points of GRP94, BiP and truncated GRP94 are shown in Figure 6D.

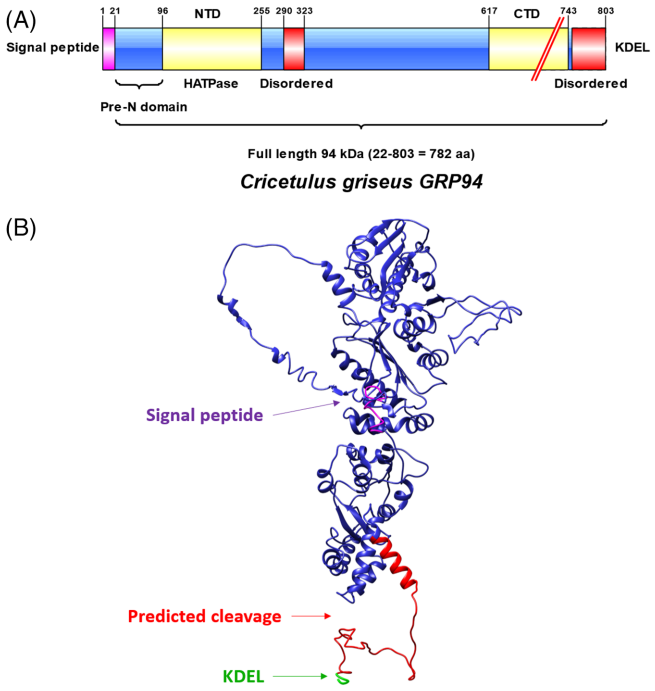

FIGURE 8 Predicted cleavage of GRP94. (A) Schematic diagram of GRP94 sequence with expected cut site. (B) Homology model of GRP94 generated using i-TASSER and colored by Chimera showing the loose acidic C-terminal of GRP94

2.7 | The small molecular weight GRP94 is devoid of its acidic C-terminal and KDEL retention motif as determined by peptide mapping

In order to confirm that the small molecular weight species of GRP94 is devoid of its KDEL motif, the full length and the truncated bands were precisely cut and sent for peptide mapping. Briefly, ER stress was induced, as mentioned above, using 5 μg/mL BFA in a culture volume of 30 mL. The sample of CHO cell lysate treated or not by BFA were run on two 8% SDS-PAGE gels, one of which was blotted onto a PVDF membrane that was later cut and probed for either GRP94 or KDEL (Figure 7A,B), while the other was stained with SYPRO Ruby protein gel stain (Figure 7C). The bands corresponding to the molecular weight of either full length GRP94 (~90-100 kDa) or truncated (~75-80 kDa) were excised and sent for peptide mapping. The detailed steps of gel cutting are shown in Figure S6. The results showed complete coverage of the full length GRP94 sample (sample 1) sequence (Figure 7D) while the truncated GRP94 (sample 2) showed coverage up until K733. No peptides were detected after A734 in the truncated GRP94 sample (Figure 7E). A comparison of the two peptide maps are shown (Figure 7E). The signal peptide (M1-A21) was not detected in either sample, indicating that this protein is a mature protein that has passed through the ER. The D22-K37 peptide is the N-terminal of the mature protein just after the signal peptide which was detected in both samples. N-terminal and middle domain peptides showed comparable abundance between the two samples. The C-terminal of truncated GRP94 was not detected while that of the full length was detected. The peptide E795-L803 (containing KDEL) was absent in the peptide map of the truncated GRP94 as shown in the zoomed view of the stacked chromatograms (Figure 7G).

A schematic diagram of GRP94 and the suggested truncated form is presented in Figure 8A. A three-dimensional model of GRP94 was constructed by i-TASSER[31] and the model representation was prepared by UCSF Chimera.[32] We suggest that the loose C-terminal and a part of the C-terminal domain are cleaved, losing the KDEL motif and thus promoting its secretion into the medium. The truncated form is slightly larger than BiP, as defined by the molecular weight (Figures 6F and S3). Comparison of peptides' intensities are shown in Figure S7A,B. The small molecular weight GRP94 species (sample 3) was detected in minor quantities in the DMSO-treated CHO cell lysate. It did not show any C-terminal peptide (Figure S7C).

2.8 | HeLa cells does not show truncation of GRP94 C-terminal upon ER stress

In order to check whether this GRP94 truncation phenomenon is shared between different mammalian cells, HeLa cells were used as a representative of human cells. HeLa cells were cultures in IMDM medium with 10% fetal bovine serum in T25 flasks. Serial concentration of either BFA or Tg was used to induce ER stress. After 24 hours of exposure, images were taken by the phase contrast mood of Keyence All-in-One fluorescence microscope (Figure 9A,B) and cells were lysed for western blot analysis. BiP showed the expected upregulation upon ER stress induction; however, GRP94 did not show any small molecular weight species (Figure 9C,D). To confirm which form of GRP94 is secreted to the medium, HeLa cells were cultured in T75 flasks, 2 days later media was discarded and the cells were washed by PBS. Then, the cells were cultured in IMDM serum free medium while treated with Tg. After 24 hours of culture in IMDM-serum free medium and Tg, cells and media were collected, the media were concentrated by ultrafiltration as usual. The western blots of cell lysates and media did not show any small molecular weight species of GRP94 as shown in (Figure 9E).

3 | DISCUSSION

In this study, we investigated the secretion of ER chaperones into extracellular medium. We serendipitously found that endogenous GRP94 is secreted into the medium as a low-molecular-weight species devoid of its ER retention motif. We also reported a comparison between GRP94 and BiP, the two most abundant proteins in the ER.[33] Both GRP94 and BiP are highly upregulated at the mRNA level during ER stress. However, BiP shows high upregulation in cell lysates, whereas both proteins are secreted into the medium upon the induction of ER stress.

We expressed KDELR1 under the BiP promoter to investigate whether the secretion of chaperones is dependent on the saturation

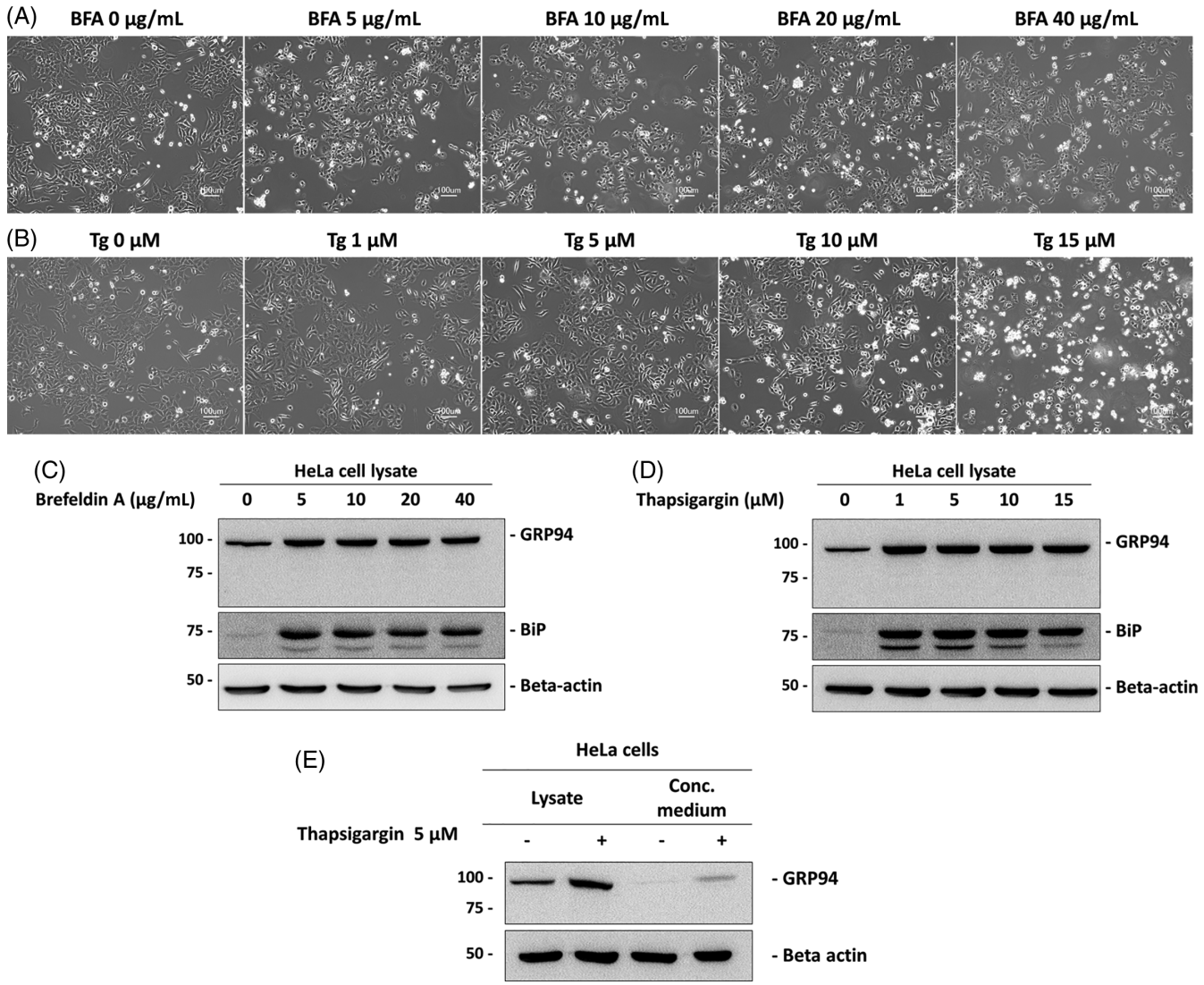

FIGURE 9 ER stress does not induce GRP94 truncation in HeLa cells. HeLa cells were grown in IMDM medium supplemented by 10% FBS. Two days after seeding, cells were treated by serial concentrations of BFA or Tg in T25 flasks. (A) Phase-contrast images of BFA-treated HeLa cells, and (B) phase contrast images of Tg-treated HeLa cells growing in T25 flasks in IMDM medium supplemented by 10% FBS after 24 hours of exposure to 0, 5, 10, 20, 40 µg/mL BFA or 0, 1, 5, 10, 15 µM Tg, respectively. (C,) Western blot of GRP94, BiP and beta-actin of BFA-treated (C) or Tg-treated (D) HeLa cells in T25 flasks. (E) Western blot of HeLa cell lysates and concentrated media after 24 hours of Tg treatment. Cells were seeded in T75 flasks, 2 days later, the cells were washed b PBS and media exchanged by IMDM serum-free media while treating the cells with or without Tg. Next day, media was harvested and concentrated by ultrafiltration. Lysate and media samples were blotted against GRP94 and beta-actin

of ER retention machinery, as reported earlier in CHO[20] and HeLa cells.[34] We report that even though KDELR1 was upregulated in our engineered model in accordance with the upregulation of ER chaperones, this still allowed the secretion of ER chaperones to the medium and improved BiP retention minimally. We suggest that the secretion of chaperones into the medium is because of masking of the KDEL motif and weak upregulation of KDEL receptors.

In contrast, GRP94 secretion was completely independent of KDELR1. It was secreted as a lower-molecular-weight species. We attempted to use different molecular techniques to check whether the KDEL motif was still present.

When the cells were treated with BFA, the secretion of ER chaperones BiP and GRP94 was inhibited. Additionally, GRP94 truncation still occurred upon BFA treatment, while co-treatment by Tg/BFA did not induce truncation. We thus suggest that GRP94 is expressed as a full-length protein; then, upon ER stress, it is truncated inside the ER by ER proteases (probably by intramembrane ER proteases).[35,36] Subsequently, it loses its acidic C-terminal and a part of its C-terminal domain, preventing its recapture from the *cis*-Golgi. This is supported by our data showing that GRP94 did not reside in the *cis*-Golgi as also found in human endothelial EAhy926 cells.[30]

It is a major challenge to conduct serum proteomic studies of proteins present at a low level. Serum proteins such as albumin and

antibodies represent the majority of proteins in serum and mask other secretory proteins.[37] In this study, we proposed an interdisciplinary approach of using suspension cells that are easily grown in shake flasks and bioreactors and adapted to serum-free conditions to bypass the difficulty of studying the secretory proteome in serum-containing medium. An important example of such cells is CHO cells, which can be used to study secretory proteins, among which we identified a truncated form of one of the most abundant ER proteins. However, whether this truncation and secretion are because of the absence of serum in the culture medium is yet to be investigated.

A novel approach in vaccine engineering is the use of a secreted form of gp96 (GRP94), in which the C-terminal retention KDEL motif is replaced by an IgG Fc-domain in vaccine cells,[29,38] leading to a secreted form of the antigen-presenting gp94-IgG complex that generates a very powerful immune response.[39] Additionally, engineered GRP94 without the KDEL motif was found to suppress tumor growth.[40] In this study, we reported that the KDEL-deprived GRP94 form may occur naturally in mammalian cells by secretion as a truncated form into the medium, or intracellularly by UPR activation.

Finally, we consider that further experiments on hamster GRP94 are required to identify proteins responsible for the proteolytic cleavage of GRP94. Studying this phenomenon will pave the road for subsequent engineering of this chaperone, which should lead to improvements in the production of difficult-to-express chimeric antibodies. Additionally, because of the high sequence homology between human and hamster GRP94s (Figure S5), we hypothesize that the reported GRP94 truncations and secretion[41] occur at the C-terminal and not the N-terminal as previously reported.[42] Nevertheless, HeLa cells did not show GRP94 truncation upon ER stress induction by either Tg or BFA. Accordingly, this phenomenon seems to be a cell specific and not a general phenomenon. It is hypothesized to be an antigen presentation pathway directing cleaved peptides from the ER to the cell exterior which will be later captured by antigen presenting cells. Since GRP94 has been proven previously to be liable to calpain degradation in-vitro in human cells[42]; therefore, this phenomenon might be a cell specific phenomenon that is triggered by certain activators or pathways. The exact disease model behind which this phenomenon functions is still unknown; whether it is tumor, inflammation, extended ER stress or DNA damage.

4 | MATERIALS AND METHODS

4.1 | Cloning of KDELR1 and PDI, and generation of a stable cell line

We used the previously constructed plasmid to generate stable CHO-K1 cells overexpressing KDELR1.[20] Similarly, PDI was cloned and overexpressed. Briefly, total RNA was extracted from CHO-K1 cells using the FastGene RNA Premium Kit (Nippon Genetics, Tokyo, Japan) followed by first-strand cDNA synthesis using the PrimeScript cDNA synthesis kit (Takara Bio, Kusatsu, Japan). PDI was PCR-amplified using the forward primer 5′-CCAGCCTCGAGAC**ATG**CTGA GCCGTTCTCTGCTG-3′ (*Xho*I site) and reverse primer 5′-GATG CGGCCGCCACCGAGGTCTTGGGTTTGGGT G-3′ (*Not*I site) and inserted into the plasmid under the CMV promoter. Stable cell lines were generated using the Neon Transfection System (Thermo Fisher Scientific, Waltham, Massachusetts).

4.2 | Batch culture of KDELR1- and PDI-overexpressing cells

CHO-K1, CHO-K1-KDELR1 and CHO-K1-PDI cell suspensions were used as models to investigate the possibility of ER saturation and secretion of chaperones into the medium. Cells were seeded in 20 mL cultures of Serum-free BalanCD CHO Growth A medium (Irvine Scientific, Santa Ana, California) containing 6 mM L-glutamine with or without 800 μg/mL G418. The cell concentration was determined using a Vi-CELL XR Cell Counter (Beckman Coulter, Brea, California). Samples were taken from harvested cells (RIPA buffer with 1% protease inhibitor) when the cell concentration reached ~50-100 × 10^5 cells/mL. To concentrate the medium, 12 mL of it was centrifuged at 10 000*g* for 2 minutes. The supernatant was then filtered using a 0.22 μm syringe filter. Next, 10 mL of this syringe-filtered supernatant was concentrated by ultrafiltration using Amicon Ultra-4 Centrifugal Filter Units, MWCO = 30 000 (Merck Millipore, Burlington, Massachusetts), at 4000 *g* for 10 minutes each cycle. The supernatant was then buffer-exchanged using 4 mL of 1× PBS.

4.3 | Western blotting

Samples were loaded onto 12% SDS-PAGE gels unless mentioned otherwise. Electrophoresed proteins were then transferred to PVDF membranes using the semi-dry method. Alternatively, some samples were loaded onto SDS-PAGE and a blotting system (Merck, KGaA, Darmstadt, Germany), wherever mentioned. The Immobilon Western Chemiluminescent HRP substrate (WBKLS0500; Merck Millipore) was used for chemiluminescent imaging using a LuminoGraph II Chemiluminescent Imaging System (ATTO, Tokyo, Japan). Band intensities were measured using CS Analyzer (ATTO).

4.4 | Antibodies and fluorophores

The primary antibodies used were β-actin [anti-β-actin mouse mAb (8H10D10, #3700; Cell Signaling Technology, Danvers, Massachusetts)], anti-BiP (rabbit Ab, 3177; Cell Signaling Technology), anti-P4hb (rabbit Ab, ab137110; Abcam, Cambridge, UK), anti-Calr (rabbit Ab, 2891; Cell Signaling Technology), anti-GRP94 (rabbit Ab, 2104S; Cell Signaling Technology), anti-GM130 (mouse Ab, 610 822; BD Biosciences, Franklin Lakes, New Jersey) and KDEL mouse antibody (2D6, MA5-27581; Invitrogen, Carlsbad, California). The secondary antibodies used were goat anti-rabbit IgG H&L Alexa Fluor

488 conjugated (ab150081; Abcam), goat anti-mouse IgG H&L Alexa Fluor 647-conjugated (ab150119; Abcam), HRP-conjugated rabbit anti-mouse IgG H&L (ab6728; Abcam) and goat anti-rabbit IgG H&L (HRP) (ab6721; Abcam). The ER was stained using the ER-ID Red assay kit, in accordance with the protocol of the manufacturer (Enzo Life Sciences, Farmingdale, New York).

4.5 | Fluorescence microscopy

Adherent CHO-K1 cells were grown in T25 flasks in IMDM (Iscove's Modified Dulbecco's Medium; Thermo Fisher Scientific) supplemented with 10% fetal bovine serum (Thermo Fisher Scientific). The cells were passaged into 12-well plates on 18 mm lysine-coated coverslips (Neuvitro Corporation, Vancouver, Washington). Two days later, the cells were washed three times with 1× PBS, fixed by 4% paraformaldehyde in 1× PBS solution for 15 minutes, quenched with 100 mM glycine/PBS for 5 minutes, followed by two washes with 1× PBS for 5 minutes each. Permeabilization was performed using 0.1% Triton X-100/PBS for 5 minutes and blocked using 3% bovine serum album in PBS. Fluorescent images of the primary antibodies used were obtained using an All-in-One Fluorescence Microscope, BZ-X710 (Keyence, Osaka, Japan). All chemicals were purchased from Fujifilm Wako (Osaka, Japan), unless mentioned otherwise.

4.6 | Cloning of BiP promoter

Genomic DNA was purified from a CHO-K1 suspension culture using the High Pure PCR Template Preparation Kit (Roche Life Science, Penzberg, Germany). The BiP promoter was amplified using the forward primer 5′-TCTCGAGCTCAAGCTTCAACCTAACCCAGCCAAAC-3′ and the reverse primer 5′-GGCGACCGGTGGATCCCTTGCCGG CGCTGTGGGC-3′ with the Q5 High-Fidelity 2× Master Mix (New England Biolabs, Ipswich, Massachusetts). The PCR product was then inserted into the pcDNA3.1-citrine plasmid[43] after digestion with *Hin*dIII and *Bam*HI. Ligation was conducted by in-fusion cloning using the In-Fusion HD Cloning Kit (Takara Bio) as per the manufacturer's protocol. The expression vector was transfected into CHO cells and the expression of citrine was examined (data not shown).

Next, the promoter was amplified from the pcDNA3.1-BiP promoter-citrine constructed plasmid using the forward primer 5′-CAGACTAGTTCAACCTAACCCAGCCAAACC-3′ (SpeI restriction site) and the reverse primer 5′-AACAAGCTTGATCCCTTGCCGGCGCTGT-3′ (HindIII restriction site). The PCR product was inserted into the previously constructed pBudCE4.1-KDELR1 plasmid[20] after removing the CMV promoter by restriction digestion with SpeI and HindIII. Then, the mock backbone (pBudCE4.1) and the constructed plasmid were linearized and used to transfect CHO-K1 cells using the Neon Transfection System (Thermo Fisher Scientific). The cells were selected with 200 μg/mL zeocin for two passages and then maintained in 100 μg/mL zeocin.

4.7 | Chemical treatments

ER stress was induced using 5 μg/mL working concentration of tunicamycin, as described previously,[20] or 1 μM working concentration of Tg unless mentioned otherwise. An equal volume of the vehicle dimethyl sulfoxide was used as a control. ER stress was induced in a suspension batch culture when the cell concentration was ~20 × 10^5 cells/mL. ER to Golgi transport was blocked by 10 μg/mL working concentration of BFA (Nacalai Tesque, Kyoto, Japan).

4.8 | RT-qPCR

RT-qPCR was performed as described previously[20] using the same primer pairs. The primers used for Hsp90aa1 were 5′-TCCCAAGACGTGCTCCATT TG-3′ (forward) and 5′-TCCTCAGAATCCACCACTCCTC-3′ (reverse).

4.9 | RT-PCR

To check whether the low-molecular-weight GRP94 is a transcript variant, ER stress was induced by tunicamycin or exposure to DMSO as a control, as mentioned earlier. Total RNA was extracted and cDNA was synthesized as mentioned earlier. Three sets of primers covering the mRNA transcript were used to investigate different PCR products under normal and stress conditions: primer set 1 (forward: 5′-TCCT GCGACCGAAGAGGACTTG, reverse: 5′-AGTGCAGGGGAGAAGGAG GCTG-3′), primer set 2 (forward: 5′-GCAGAGAAGGCTCAAGGAC AGATG-3′, reverse: 5′-TTTCCTGCTTGACCCAGCCATGAA-3′) and primer set 3 (forward: 5′-GCTTGGTGTGATTGAGGACCACTC-3′, reverse: 5′-TGTCTTCAGGCTCTTCTTCCGGTT-3′). The PCR products were subjected to agarose gel electrophoresis.

4.10 | Immunoprecipitation

IP of GRP94 was performed using cell lysates or concentrated media of CHO cells grown in suspension batch cultures. The volume of the sample was adjusted to 500 μL with cell extraction buffer and incubated with 5 μL of the anti-GRP94 polyclonal antibody (rabbit, ab227293; Abcam) for 2 hours on a rotary shaker at room temperature or overnight at 4°C. The sample was then incubated with 50 μL of Dynabeads magnetic protein G beads (Thermo Fisher Scientific) for 1 hour at room temperature. Magnetic protein G beads were pulled down by a magnet, washed three times with 1× PBS, and eluted with 25 μL of 50 mM glycine (pH = 2.8). For western blot, VeriBlot for IP detection reagent (HRP) (ab131366, Abcam) was used to minimize the interference of IP antibody.

4.11 | Mass spectroscopy

Cell lysates of DMSO-treated or BFA-treated CHO-K1 cells were run on 8% conventional gels and stained by SYPRO Ruby protein gel stain

(Thermo Fisher Scientific). Bands corresponding to a molecular weight around 75 or 100 kDa were manually cut out and sent for analysis by timsTOF Pro (Bruker, Billerica, Massachusetts). In-gel digestion by trypsin, de-staining and reduction by alkylation were performed prior to the run. A database search was performed using the TrEMBL database against Chinese hamster (*Cricetulus griseus*).

4.12 | 2D gel electrophoresis

DMSO-treated or BFA-treated CHO-K1 cell lysates were precipitated with trichloroacetic acid, washed with acetone and resuspended in rehydration solution. The sample was run on Auto 2D plus (Merck) on 7.5% gel and a chip of pH range of 3-10. The gel was transferred to a PVDF membrane and blotted against anti-KDEL antibody as previously mentioned. It was then stripped using low-pH stripping solution, washed, reblocked, incubated with anti-GRP94 antibody and visualized.

4.13 | HeLa cell culture

HeLa cells were grown in IMDM medium (17633-10L, Sigma Aldrich) supplemented with 10% fetal bovine serum (FBS, Sigma Aldrich). Cultures were grown in T25 or T75 flasks in static incubator at 37° and 5% CO_2.

4.14 | Statistical analysis

The normalized values of either western blot band intensity or RT-qPCR gene expression were compared using Tukey's multiple comparison test using GraphPad Prism (GraphPad Software, San Diego, California). $P < .05$ was considered to represent a statistically significant difference. Bars represent means and error bars represent SDs.

ACKNOWLEDGMENTS

This research was supported by the Developing Key Technologies for Discovering and Manufacturing Pharmaceuticals Used for Next-Generation Treatments Program (Japan Agency for Medical Research and Development: AMED) under grant numbers JP17ae0101003, JP20ae0101056, JP20ae0101057, JP20ae0101058 and JP20ae0101066, and MEXT/JSPS KAKENHI (grant number JP17H06157). Andrew Samy was supported by a Japanese government (Monbukagakusho: MEXT) scholarship. We sincerely thank Professor Susumu Uchiyama and Dr Kentaro Ishii (Osaka University) for the analysis of MS and fruitful discussions and comments. We are also grateful to Merck for providing us with a two-dimensional electrophoretic device, Auto2D Plus and related consumables. We also thank Mr Masayuki Kosugi, Mr Kimihiko Yabe and Ms Sayuri Otaki for useful discussions. Finally, we thank the Edanz Group (https://en-author-services.edanz.com/ac) for editing a draft of this manuscript.

CONFLICT OF INTEREST

The authors declare that they have no conflicts of interest.

AUTHORS' CONTRIBUTIONS

Andrew Samy designed the study, performed most of the experiments and prepared the manuscript and figures. Noriko Yamano-Adachi, Yuichi Koga and Takeshi Omasa supervised the study. All authors have read and approved the final version of this manuscript.

PEER REVIEW

The peer review history for this article is available at https://publons.com/publon/10.1111/tra.12818.

ORCID

Andrew Samy https://orcid.org/0000-0001-9152-1327
Noriko Yamano-Adachi https://orcid.org/0000-0002-2167-5379
Yuichi Koga https://orcid.org/0000-0003-1702-6488
Takeshi Omasa https://orcid.org/0000-0003-0635-3862

REFERENCES

1. Dubey A, Prajapati KS, Swamy M, Pachauri V. Heat shock proteins: a therapeutic target worth to consider. *Vet World*. 2015;8:46-51.
2. Marzec M, Eletto D, Argon Y. GRP94: an HSP90-like protein specialized for protein folding and quality control in the endoplasmic reticulum. *Biochim Biophys Acta*. 2012;1823:774-787.
3. Knowlton AA, Salfity M. Nuclear localization and the heat shock proteins. *J Biosci*. 1996;21:123-132.
4. Miller DJ, Fort PE. Heat shock proteins regulatory role in neurodevelopment. *Front Neurosci*. 2018;12:821.
5. Huck JD, Que NL, Hong F, Li Z, Gewirth DT. Structural and functional analysis of GRP94 in the closed state reveals an essential role for the pre-N domain and a potential client-binding site. *Cell Rep*. 2017;20:2800-2809.
6. Johnson JL. Evolution and function of diverse Hsp90 homologs and cochaperone proteins. *Biochim Biophys Acta Mol Cell Res*. 2012;1823:607-613.
7. Luo B, Lee AS. The critical roles of endoplasmic reticulum chaperones and unfolded protein response in tumorigenesis and anticancer therapies. *Oncogene*. 2013;32:805-818.
8. Huard DJE, Jonke AP, Torres MP, Lieberman RL. Different Grp94 components interact transiently with the myocilin olfactomedin domain in vitro to enhance or retard its amyloid aggregation. *Sci Rep*. 2019;9:1-12.
9. Dollins DE, Warren JJ, Immormino RM, Gewirth DT. Structures of GRP94-nucleotide complexes reveal mechanistic differences between the hsp90 chaperones. *Mol Cell*. 2007;28:41-56.
10. Immormino RM, Dollins DE, Shaffer PL, Soldano KL, Walker MA, Gewirth DT. Ligand-induced conformational shift in the N-terminal domain of GRP94, an Hsp90 chaperone. *J Biol Chem*. 2004;279:46162-46171.
11. Argon Y, Bresson SE, Marzec MT, Grimberg A. Glucose-regulated protein 94 (GRP94): a novel regulator of insulin-like growth factor production. *Cell*. 2020;9:1844.
12. Christianson JC, Shaler TA, Tyler RE, Kopito RR. OS-9 and GRP94 deliver mutant α1-antitrypsin to the Hrd1-SEL1L ubiquitin ligase complex for ERAD. *Nat Cell Biol*. 2008;10:272-282.
13. Nishitoh H. CHOP is a multifunctional transcription factor in the ER stress response. *J Biochem*. 2012;151:217-219.
14. Torres M, Akhtar S, McKenzie EA, Dickson AJ. Temperature downshift modifies expression of UPR-/ERAD-related genes and enhances

production of a chimeric fusion protein in CHO cells. *Biotechnol J*. 2020;16:2000081.
15. Zhu G, Lee AS. Role of the unfolded protein response, GRP78 and GRP94 in organ homeostasis. *J Cell Physiol*. 2015;230:1413-1420.
16. Liu B, Staron M, Hong F, et al. Essential roles of grp94 in gut homeostasis via chaperoning canonical Wnt pathway. *Proc Natl Acad Sci U S A*. 2013;110:6877-6882.
17. Chong LP, Wang Y, Gad N, Anderson N, Shah B, Zhao R. A highly charged region in the middle domain of plant endoplasmic reticulum (ER)-localized heat-shock protein 90 is required for resistance to tunicamycin or high calcium-induced ER stresses. *J Exp Bot*. 2015;66:113-124.
18. Omasa T, Takami T, Ohya T, et al. Overexpression of GADD34 enhances production of recombinant human antithrombin III in Chinese hamster ovary cells. *J Biosci Bioeng*. 2008;106:568-573.
19. Onitsuka M, Kinoshita Y, Nishizawa A, Tsutsui T, Omasa T. Enhanced IgG1 production by overexpression of nuclear factor kappa B inhibitor zeta (NFKBIZ) in Chinese hamster ovary cells. *Cytotechnology*. 2018;70:675-685.
20. Samy A, Kaneyoshi K, Omasa T. Improvement of intracellular traffic system by overexpression of KDEL receptor 1 in antibody-producing CHO cells. *Biotechnol J*. 2020;15(6):1900352.
21. Yamano-Adachi N, Ogata N, Tanaka S, Onitsuka M, Omasa T. Characterization of Chinese hamster ovary cells with disparate chromosome numbers: reduction of the amount of mRNA relative to total protein. *J Biosci Bioeng*. 2020;129:121-128.
22. Vodopivec M, Lah L, Narat M, Curk T. Metabolomic profiling of CHO fed-batch growth phases at 10, 100, and 1,000 L. *Biotechnol Bioeng*. 2019;116:2720-2729.
23. Alden N, Raju R, McElearney K, et al. Using metabolomics to identify cell line-independent indicators of growth inhibition for Chinese hamster ovary cell-based bioprocesses. *Metabolites*. 2020;10(5):199.
24. Gupta SK, Srivastava SK, Sharma A, et al. Metabolic engineering of CHO cells for the development of a robust protein production platform. *PLoS One*. 2017;12:e0181455.
25. Yamano N, Takahashi M, Ali Haghparast SM, et al. Increased recombinant protein production owing to expanded opportunities for vector integration in high chromosome number Chinese hamster ovary cells. *J Biosci Bioeng*. 2016;122:226-231.
26. Maldonado-Agurto R, Dickson AJ. Multiplexed digital mRNA expression analysis profiles system-wide changes in mRNA abundance and responsiveness of UPR-specific gene expression changes during batch culture of recombinant Chinese hamster ovary cells. *Biotechnol J*. 2018;13:1700429.
27. Prashad K, Mehra S. Dynamics of unfolded protein response in recombinant CHO cells. *Cytotechnology*. 2015;67:237-254.
28. Murshid A, Gong J, Calderwood SK. The role of heat shock proteins in antigen cross presentation. *Front Immunol*. 2012;3:63.
29. Strbo N, Podack ER. Secreted heat shock protein gp96-Ig: an innovative vaccine approach. *Am J Reprod Immunol*. 2008;59:407-416.
30. Paris S, Denis H, Delaive E, et al. Up-regulation of 94-kDa glucose-regulated protein by hypoxia-inducible factor-1 in human endothelial cells in response to hypoxia. *FEBS Lett*. 2005;579:105-114.
31. Roy A, Kucukural A, Zhang Y. I-TASSER: a unified platform for automated protein structure and function prediction. *Nat Protoc*. 2010;5:725-738.
32. Pettersen EF, Goddard TD, Huang CC, et al. UCSF chimera—a visualization system for exploratory research and analysis. *J Comput Chem*. 2004;25:1605-1612.
33. Itzhak DN, Tyanova S, Cox J, Borner GHH. Global, quantitative and dynamic mapping of protein subcellular localization. *Elife*. 2016;5:e16950.
34. Llewellyn DH, Roderick HL, Rose S. KDEL receptor expression is not coordinatedly up-regulated with ER stress-induced reticuloplasmin expression in HeLa cells. *Biochem Biophys Res Commun*. 1997;240:36-40.
35. Wolfe MS. Intramembrane-cleaving proteases. *J Biol Chem*. 2009;284:13969-13973.
36. Verhelst SHL. Intramembrane proteases as drug targets. *FEBS J*. 2017;284:1489-1502.
37. Wang H, Hanash S. Intact-protein based sample preparation strategies for proteome analysis in combination with mass spectrometry. *Mass Spectrom Rev*. 2005;24:413-426.
38. Podack ER, Raez LE. Allogeneic tumor-cell-based vaccines secreting endoplasmic reticulum chaperone gp96. *Expert Opin Biol Ther*. 2007;7:1679-1688.
39. Strbo N, Garcia-Soto A, Schreiber TH, Podack ER. Secreted heat shock protein gp96-Ig: next-generation vaccines for cancer and infectious diseases. *Immunol Res*. 2013;57:311-325.
40. Baker-LePain JC, Sarzotti M, Fields TA, Li CY, Nicchitta CV. GRP94 (gp96) and GRP94 N-terminal geldanamycin binding domain elicit tissue nonrestricted tumor suppression. *J Exp Med*. 2002;196:1447-1459.
41. Trychta KA, Bä S, Henderson MJ, et al. KDEL receptors are differentially regulated to maintain the ER proteome under calcium deficiency. *Cell Rep*. 2018;25:1829-1840.
42. Reddy RK, Lu J, Lee AS. The endoplasmic reticulum chaperone glycoprotein GRP94 with Ca2+− binding and antiapoptotic properties is a novel proteolytic target of calpain during etoposide-induced apoptosis. *J Biol Chem*. 1999;274:28476-28483.
43. Griesbeck O, Baird GS, Campbell RE, Zacharias DA, Tsien RY. Reducing the environmental sensitivity of yellow fluorescent protein. *J Biol Chem*. 2001;276:29188-29194.

SUPPORTING INFORMATION

Additional supporting information may be found in the online version of the article at the publisher's website.

How to cite this article: Samy A, Yamano-Adachi N, Koga Y, Omasa T. Secretion of a low-molecular-weight species of endogenous GRP94 devoid of the KDEL motif during endoplasmic reticulum stress in Chinese hamster ovary cells. *Traffic*. 2021;22(12):425-438. doi:10.1111/tra.12818